Model study of organic carbon attenuation and oxygen mass transfer in persistent

- 2 aggregate layers in the deep sea
- 3 Timothy J. Shaw^{a*}, Corrianna Boucher^a, Christine L. Huffard^b, Kenneth L. Smith Jr.^b,

4

1

- 5 a University of South Carolina, Columbia, SC 29208
- 6 b Monterey Bay Aquarium Research Institute, Moss Landing, CA 95039

7 8

ABSTRACT

9 10

11

12

13

14

15

16

17

18

19

20

21

22

23

24

25

26

27

28

29

30

31

A time series study from 1989-2017 indicates that, increasingly, carbon export to abyssal sediments in the California Current Ecosystem (CCE), 220 km west of the central California coast (Sta. M), occurs as rapidly sinking pulses of particulate organic carbon (POC). Nearly continuous sediment trap collections confirm that POC export to 3400 meters increased significantly after 2011 with carbon attenuation (as fraction of POC remineralized) ranging from a low of 57% to a high of 77% during periods of pulsed flux. All of the major pulse events for the period resulted in the delivery of detrital aggregates that covered part or all of the sediment surface as an organic carbon rich layer at ~4000 m depth. However, the magnitude of the measured Sediment Community Oxygen Consumption (SCOC) did not increase proportionally to the organic carbon inventory change. Here, a model of oxygen consumption informed by the time series data at Sta. M in the CCE suggest that aggregate flocs constitute a major source for benthic carbon and a barrier to mass transport of oxygen to surface sediments leading to increased carbon attenuation in surface sediment layers. The correlation of POC delivery with aggregate coverage shows that the majority of POC delivery during pulse events is likely to consume all of the oxygen within the aggregates. Results indicate that an increasing fraction of POC reaching the abyssal sediments at Sta. M under conditions that support increased net burial of carbon.

This finding is significant in the context of the fraction of the total POC flux that occurs as pulse events in this important upwelling region. During the period from 2011-2017, a third of the total POC flux resulted in aggregate flocs that covered a significant portion of the sediment surface (>47%). Following the 2015-2016 El Nino period the flocs became a dominant feature of the sediment surface. More than 80% of the POC flux to near bottom sediment traps in 2017

- occurred coincident with aggregate floc cover of more than 90% of the sediments. The resultant
- 33 physical barrier to oxygen transport and relatively low consumption of newly delivered carbon
- indicate conditions that are more typical of environments having low oxygen bottom waters.
- 35 Keywords
- 36 Carbon attenuation; Carbon pump; Detrital aggregates; Sediment redox; Sediment community
- 37 oxygen consumption
- 38 *Corresponding author.
- 39 E-mail address: shaw@mailbox.sc.edu (T.J. Shaw)

1. Introduction

- Global estimates of the delivery of phytodetritus to the deep ocean, as Particulate Organic
- Carbon (POC) burial, put an upper limit on the efficiency of the "Carbon Pump" on the order of
- 45 5-15% (Laws et al., 2000; Giering et al., 2014). However, episodic productivity events
- 46 associated with transient physical processes are becoming more frequent and, in turn, their
- 47 impact on the transfer of organic carbon from the upper ocean to abyssal depths has become
- 48 more significant (Smith et al., 2013, 2018; Stukel et al., 2017). Ephemeral oceanographic
- 49 processes like upwelling events, fronts, eddies and filaments lead to productivity events that
- export particulate carbon out of surface waters as pulses. The physical dynamics of these systems
- can enhance both primary production and vertical transport by processes such as direct
- 52 subduction of particles and enhanced aggregation. For example, in the CCE, carbon export as
- subduction in proximity to fronts can be 2-3 times higher than gravitational sinking of POC
- 54 (Stukel et al., 2017). In addition, the characteristic physical dynamics of these systems are
- critical to mediating particle aggregation/coagulation and rapid settling (Kiorboe et al., 1996).
- These and similar processes support the delivery of pulses of fresh phytodetritus to the sea floor
- at abyssal depths (Agusti et al., 2015). Pulses of large, rapidly sinking organic rich particles
- 58 appear to be less susceptible to carbon flux attenuation during transit from surface waters,
- 59 supporting lower attenuation as increased carbon delivery to the abyssal sediments (Hammond et
- al., 1996; Baldwin et al., 1998; Shaw et al., 1998; Buesseler 1998; Lampitt et al., 2009, 2010;
- 61 Riley et al., 2012; Buesseler et al., 2008; Buesseler and Boyd, 2009; Smith et al., 2018, 2013).
- This is consistent with reduced rates of mineralization of labile carbon fractions at lower
- 63 temperatures as particles settle to the cooler midwater depths (Marsay et al., 2015). The impact

of the magnitude and physiochemical form of these pulses of POC on carbon attenuation at the sea floor is the focus of this study.

Studies combining sediment traps and time-lapse camera systems in the California Current Ecosystem (CCE) verify that pulses of POC to the benthos are increasing in number and intensity (Smith et al., 1998, 2018, 2013). Results from a 30-year time series show that pulse events represent an increasing fraction of the total carbon reaching the abyssal sea floor (Smith et al., 2018). Yet, the sediment community response to the pulse events, as sediment community oxygen consumption (SCOC) measured with benthic chambers, is not proportional to the pulse intensity (Smith et al., 2018). This result is surprising considering that the elapsed time between the surface water export flux and POC delivery to abyssal depths is nearly synoptic in some cases. These events were accompanied by the often-complete coverage of the sea floor with detrital aggregate (DA) flocs. The rapid flux of POC indicated by the temporal coupling of pulse events between the surface and sea floor indicate conditions that may lead to reduced carbon remineralization in the water column and increased net C burial at the sea floor.

The remineralization of Organic Carbon (Org C) with oxygen at the sea floor can be mediated by two factors that are characteristic of pulses of POC in the water column, aggregate size and microbial degradation rates. The size of aggregates is a critical factor in settling rate, and in turn, the associated rapid transit time of large particles would seem likely to support a higher fraction of surface export flux deposited as POC during pulse events depending on particle reactivity. A study of settling particle composition at similar depths (>4000 m) in the North Atlantic provides support for this assumption where particles richer in 'labile components' were associated with high flux periods (Kiriakoulakis et al., 2001). Lampitt (1985) monitored sediments at the base of the continental slope in the Eastern North Atlantic using photographs taken daily over the course of a year. He observed the rainout of a very rapidly degraded flocculent material that blanketed the sediments for several months of the year. Lampitt (1985) described the material as phytodetritus consisting of particles as large as 0.4 centimeters which can be broken down in a matter of days. These results seem to conflict with the apparent low POC and DA reactivity based on the limited SCOC response to pulse events at Sta. M (Smith et al., 2018).

Studies of carbon degradation in water column aggregates report sustained microenvironments where size and composition impact particle redox gradients (Alldredge and

Cohen, 1987; Ploug et al., 1997; Ploug et al., 2007). Microsensor studies have demonstrated the role of impedance to mass transfer into aggregates in maintaining physiochemical gradients for parameters like oxygen and diffusivity (Alldredge and Cohen, 1987; Ploug et al., 1997; Ploug et al., 2008). The measurement of persistent microscale oxygen gradients in the precursor material of aggregate flocs (i.e. marine snow, fecal pellets) reflects both rapid carbon degradation and limitation of oxygen mass transfer. A persistent gradient implies that carbon turnover rates within even sub millimeter scale particles are rapid compared to the supply of oxygen by advective or diffusive processes (Ploug et al., 2008; Alldredge and Cohen 1987). The restriction of oxygen supply to particle interiors is also a function of the thickness of the boundary layer that defines the transition from advective to diffusive controlled mass transport (Alldredge and Cohen, 1987; Ploug et al., 1997). These physical and chemical factors are likely to have an amplified impact on mass transfer as particles accumulate to produce aggregate floc layers at the sediment water interface.

Model and laboratory studies have demonstrated that sinking porous aggregates can maintain sharp chemical gradients across particle surfaces in high flow (Lehto et al., 2014; Steif et al., 2016; Moradi et al., 2018). Aggregate size, fluid flow around/through falling particles, and diffusive versus advective conditions are critical variables affecting the availability of oxygen to the particle microbiome (Alldredge and Cohen, 1986). These factors are interrelated and closely linked to aggregation and disaggregation of particles (Goldthwait et al., 2005). Settling rate plays a role in the advection of fluid around particles and is a function of particle size, shape and density (Ploug et al., 2008). Advection, in turn, regulates the availability of oxygen to the surface and, in the case of porous particles, the interior of particles (Ploug et al., 2008; Moradi et al., 2018). These factors are important in the context of this study, because their impact changes dramatically as particles settle on the sediment surface. As particles settle on a surface, the area over which chemical fluxes occur is reduced, leading to reduced chemical exchange with the particle interior and potential for the development of anoxic microenvironments (Lehto et al., 2014; Plough and Jorgensen 1999). At Sta. M, the rate at which phytodetritus is delivered to abyssal depths, as an indicator of "particulate age", does not seem to predict Org C reactivity (Smith et al., 2018). The critical question to be answered here is whether SCOC and DA inventories can be predictors of delivery and attenuation of the Org. C pulses to the sea floor. This question is addressed through a combination of synthesis of additional data from Sta. M and a model of oxygen mass transport into aggregates and surface sediments. The results should elucidate processes that affect the net sequestration of atmospheric CO₂ in abyssal sediments as a result of major productivity events.

2. Results

The data used in this study were collected as part of a near continuous >30-year time series study in the California Current Ecosystem (CCE) centered at 34°50'N, 123°00'W (Sta. M). The data were supplemented by results from ancillary studies at or near Sta. M. The data were collected using a number of methods and instruments that have, in some cases, evolved to provide better data quality and higher sampling resolution in the latter part of the time series. The free-vehicle grab respirometer (FVGR) and time-lapse camera tripod systems that were used early in the time series have been replaced by an autonomous benthic Rover (Smith et al., 2017). The primary data types used in this study were, POC flux collected from sediment traps set at 600 and 50 meters above the bottom (mab) (Baldwin et al., 1998), SCOC and imaging measured with near daily resolution by the Rover. Translation of the image data into sediment OrgC inventories used data from samples collected using the ALVIN submersible (Smith et al., 1998).

2.1. Sta. M water column POC attenuation and reactivity

The impact of pulse events on carbon burial is a function of the attenuation of the export flux of POC and reactivity of that POC on the sea floor. Smith et al. (2018), used satellite color based estimates of the Export Flux (EF) and sediment trap POC flux to identified coupled pulses of detritus reaching abyssal depths. Those data provide an estimate of the water column attenuation and the reactivity of the POC can be calculated using the lag time assuming first order decay (Table 1). The fraction of the EF pulse that is remineralized during transit from 100 m to 3400 m (the sediment trap depth) ranges from 57%-77% (Table 1). The calculated first order decay constant based on transit time through the water column (lag time) provides an indication of the reactivity of the remineralized POC with half-lives ranging from 3-19 days (Table 1). The calculated half-lives of the pulse material would seem to predict rapid remineralization of the pulse at the sea floor, contrary to measured SCOC. The predicted water column remineralization rates, as rapid attenuation, would be biased when sediment traps "under

sampled" large pulses POC. Under sampling can result from clogging of the trap mouth and/or funnel as well as overfilling of the cup during large DA flux events like those documented between 2011-2018 (Smith et al., 1998, 2018). A decadal scale record of the ratio between POC flux (food supply) and sediment community oxygen consumption (SCOC) showed that ~ 37% of incoming POC flux was probably missed by sediment traps (Smith et al., 2016).

Investigations using time-lapse imagery of the sea floor have helped quantify pulses of POC flux missed by sediment traps as inventories of organic carbon associated with aggregates (Smith et al., 1998). For this study, high resolution imagery taken with the Rover (synoptic with SCOC measurements) was used to generate semiquantitative data on the delivery of aggregate organic carbon, the resultant inventory, and the lifetime of that material at the sediment water interface as defined by the pulse events (Table 1). It is important to note that significant DA coverage (>47%) in 2017 persisted from 1 May to the end of the sample collection period on 12 November.

2.2. Data synthesis: Organic C inventory, input and decay at the sea floor

2.21. Aggregate Organic C inventory

A method for measuring aggregate POC contributions to the sea floor was used by Smith et al. (1998) based on direct measure of the physiochemical properties of collected DA and image processing for two pulse events at Sta. M in 1994. Here we use the average compositions determined for the aggregates collected then (n=138) and the high-resolution imagery of sediment coverage measured with the Rover for recent pulse events at Sta. M. The inventories were calculated based on the average volume for individual aggregates, the number of aggregates per unit area, and the average organic C concentration per unit volume (Smith et al., 1998). The average concentration per unit volume was very similar between the two events (0.34 mg C cm⁻³ and 0.37mg C cm⁻³). The average aggregate volume and area measured from individual aggregates during the 1994 pulse events was used to determine an average aggregate layer height for later periods of high aggregate coverage (Smith et al., 1998; 2018; unpublished ROVER data). The volume to area measurements from the 1994 was consistent with an aggregate layer with vertical dimensions typically greater than 1 cm in thickness. The fraction of aggregate cover provides an aggregate volume that is translated into a aggregate Org C inventory. Figure 1 shows

lab images of cores collected for consecutive years during Fall cruises from 2016-2018. While not high resolution, the images show aggregate layers as somewhat darker, flocculent material overlying lighter, more consolidated sediments. In cores B and C there is evidence of some consolidation of the darker layer at the base of the aggregate layer suggesting compaction. The dimensions observed are consistent with measurements for the 1994 event, but the coverage is much more complete, reflecting a continuous layer rather than individual aggregates.

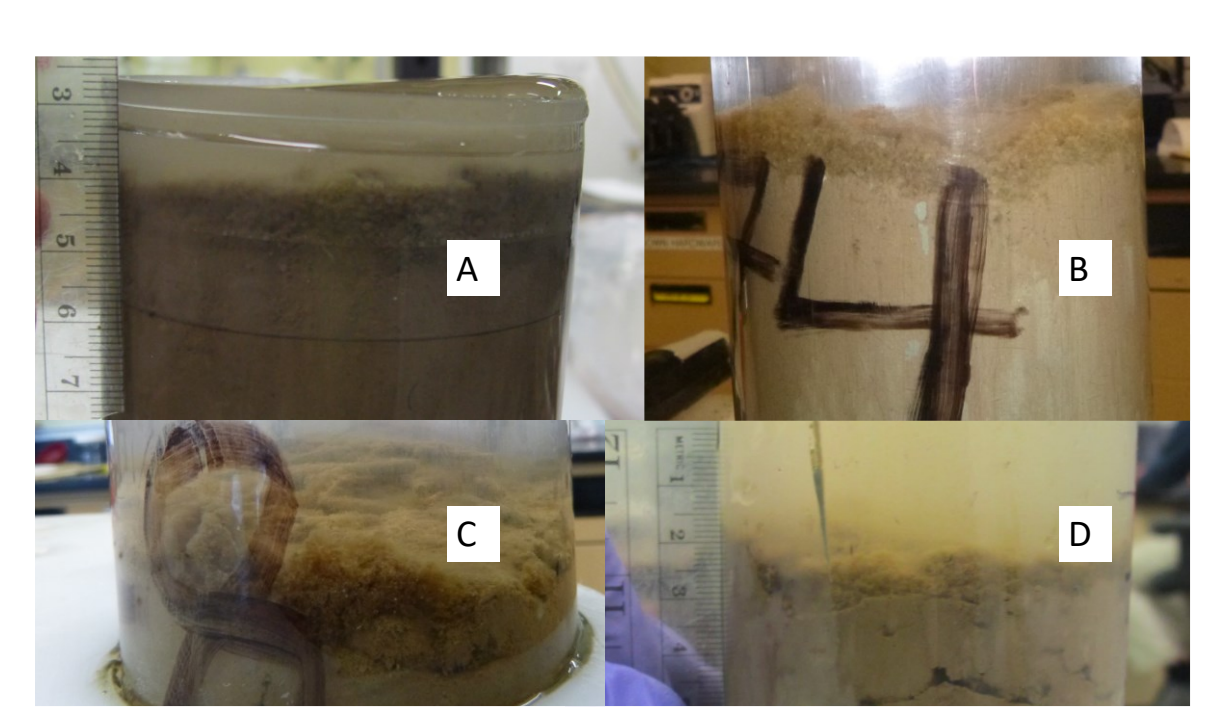


Fig. 1. Examples of aggregates recovered from Sta. M showing aggregate layer dimensions from three consecutive Fall cruises. All images are for push cores collected using the ROV Doc Ricketts. The core shown in Fig. 1A was collected on 10 Nov 2016; Fig. 1B on 20 October 2018; in Fig. 1C on 11 Nov 2017; and Fig. 1D on 10 Nov 2016. Cores in Figures 1A and 1D were collected during Pulse 4, and the Core in Fig. 1C was collected during Pulse 6 (Table 1).

The data and approach used here to calculate aggregate Org C inventories for the period between 2011 and 2017 were similar to those used by Smith et al., 1998. The same mean Org C concentrations per unit volume were used, and the volume was estimated by the % area aggregate coverage during periods when coverage was assigned to pulse events (typically >47% coverage after Smith et al., 2018). A very conservative estimate of average floc thickness of 0.5 cm was used as a minimum based on photographic evidence from recovered cores (see Fig. 1).

This is less than half of the typical volume to area measured by Smith et al. (1998) and is presented as the low end of the inventory range, and a minimum in terms of POC delivery to the sea floor during the event. During periods of near complete coverage observed for the pulse events in 2012, 2016, and 2017, the calculated inventories for events 1, 4, and 6 agree with the trap fluxes to within +/-30% (Table 1). For pulse events 2, 3, and 5, the DA delivery to the sea floor is 2-3 times greater than that collected in the sediment traps. Events 2, 3, and 5, all showed the minimum lag time between the onset of the EF event and the appearance of the DA pulse at the sea floor.

2.2.2. Sea floor carbon attenuation and reactivity

The calculated EF attenuation at the sea floor was calculated based on the difference between the integrated EF for each pulse and the calculated inventory (Table 1). The lowest attenuations were for events 2, 3, and 5 (53%-10%), while events 1, 4 and 6 showed attenuation similar to that measured for the water column (79%-73%). The reactivity of the aggregate carbon was calculated using the integrated SCOC over the pulse duration (from Smith et al., 2018) and the DA inventory assuming first order decay. The decay rates are expressed in half-life for the DA to simplify comparison to water column results. While the DA inventory indicates lower attenuation than the trap data (half lives in the water column from 3-19 days), the calculated reactivity based on SCOC (half-lives from 46-129 days) suggests lower reactivity for the DA material and underlying sediments. These two data sets offer very different conclusions for the importance of pulse events on net carbon burial at the sea floor.

The measured percentage of organic carbon in the aggregates and trap collected POC (typically 5% and above, Smith et al., 1998, 2018) suggests a Org C rich material compared to the surface sediments at Sta. M (~2%; Cai et al., 1995). Yet, the measured SCOC and calculated decay rates for the aggregate Org C, do not indicate an easily metabolized C fraction. Similarly, the rate that aggregates become visibly undetectable based on high resolution imaging suggests high remineralization rates for the associated Org C (after Lampitt 1985). Several studies report high remineralization rates for phytodetritus associated with rapid sedimentation of aggregate flocs (Hammond et al., 1995; Witbaard et al., 2000). In contrast, half lives for C ranging from 126 to 69 days (0.0055-0.10d⁻¹) for the Equatorial Pacific (Hammond et al., 1995) are consistent with the pulse events calculated here (Table 1) and estimated for Sta. M in other studies (Dunlop

et al., 2016). The low end of the rate estimates are similar to rates based on pore water gradients in aggregate free sediments prior to 2011 at Sta. M (0.004d⁻¹; Cai et al., 1995). The implication of the lower attenuation and apparent lower reactivity of the C associated with the DA flux is that higher net C burial is associated with pulse events.

Smith et al., (1998) did not find a large difference in SCOC in aggregate covered sediments compared to underlying sediments once aggregates were no longer visible. This indicates that the change in aggregate volume is not proportional to the change in Org C content as rapid remineralization. Some studies have shown that macrofauna and megafauna can account for significant consumption of DA (Bett et al, 2001). However, high resolution images and the results from previous studies do not indicate that macrofauna/megafauna grazing account for significant consumption of Org C at Sta. M (Lauerman et al., 1997; Lauerman and Kaufman, 1998). Thus, carbon delivered as DA may persist long after aggregates are no longer visible. This is consistent with the differences in aggregate porosity (>99%) compared to surface sediments (~80%; Smith et al., 1998; Cai et al., 1995). The volume change indicates a sharp increase in organic C concentration with depth through the aggregates even while the net carbon inventory decreases. This physical change may well have a larger impact on SCOC than carbon reactivity. Hammond et al., (1995) found that 70-90% of the oxygen consumption occurred in the upper 0.4 cm of sediments and was attributed to labile carbon associated with phytodetritus. Boetius et al., (2013) found that pulses of phytodetritus associated with Arctic sea-ice melt drove rapid shoaling of the oxygen penetration depth to a few mm in normally oxic sediments. The model presented below was designed to identify conditions that lead to convergence between measured SCOC, Org C delivery and porosity gradients associated with pulses of aggregates on the sediment surface. The model results return a predicted depth of oxygen penetration during conditions of aggregate cover as an indicator of sediment redox conditions.

2.3. Model assumptions and execution

240

241

242

243

244

245

246

247

248

249

250

251

252

253

254

255

256

257

258

259

260

261

262

263

264

265

266

267

268

269

The organic carbon and oxygen consumption models were designed to allow a sensitivity test for factors which influence oxygen utilization within aggregate flocs and in the underlying sediments. The strong seasonality and increased frequency in aggregate deposition at Sta. M combined with the large database provide a number of constraints for aggregate inventory and composition as presented in section 2.2 above that inform model organic carbon profiles. The

carbon and oxygen models were constrained by the following physical and chemical parameters presented in Table 2.

The calculated organic C inventories and measured SCOC were used to calculate the degradation

273 rates for the aggregate layer. For simplicity, the model tested single values for carbon

degradation rate that were on the same order as the calculated net rate for Sta. M (see Table 1).

As noted earlier these rates fall in the range of pore water based rates for Sta. M in other studies

276 (Cai et al., 1995; Dunlop et al., 2016).

275

277

278

279

280

281

282

283

284

285

286

287

288

289

290

291

292

293

294

295

296

297

298

299

300

2.3.1. First order carbon model parameters and assumptions

The carbon model parameterization reflects constraints imposed by the available data for aggregates collected at Sta. M. primarily high resolution SCOC data and images collected synoptically from the ROVER instrument. Synthesis of image data into inventories were informed by previous direct measurement of organic composition of aggregates, ranging from 3.3-142 umol cm⁻³ at Sta. M (Smith et al., 1998). A narrower range about the mean was used to inform the model of carbon degradation and constrain results based on measured SCOC (Smith et al., 1998; Smith et al., 2018). The model of carbon degradation uses a single rate, taken as a range between "refractory" and "semi-labile" Org C fractions used in previous studies and current calculations (Table 1). Measurement on individual aggregates made by Smith et al., (1998) provide a range of organic carbon concentrations for aggregates (as moles C cm⁻³). The available data were used to estimate initial porosity in aggregates based on measured volume, dry weight, and a conservative density estimate of 1.2 yields porosities higher than 99%. This is consistent with density measurements of marine snow (Prairie et al., 2015). The "disappearance" of the visible floc layer at the end of each pulse event was interpreted as a collapse of the aggregate volume rather than decay of the aggregate material. A volume decay parameter was included in the model and was constrained by the timescale for aggregate "disappearance". Parameters for initial and final volumes were constrained by the initial aggregate porosity (>99%) and porosity measurements for background sediments at Sta. M (~80%; Cai et al., 1995).

The organic carbon aggregate profile, as concentration, is generated as the first-order decay of Org C (in moles) divided by volume which is determined as a separate, faster first-order decay. The volume decay rate was taken as a first order decay and constrained by porosity data (see above). The model neglects bioturbation. The model parameters span the range of conditions presented in Table 2. The model assumes that once the aggregate layer is established,

301 aggregate carbon input is constant for the remainder of the pulse event. A comparison of total 302 mass/unit volume measurements for aggregates from Smith et al., (1998) and porosity 303 measurements for underlying sediments (Cai et al., 1995) suggest that aggregate volume is 304 reduced by a factor of >50 from the time of deposition to the disappearance of visible aggregates. 305 For the degradation rates used for the Org C fraction, the loss of volume results as aggregate age 306 exceeds the loss of organic carbon by decay, thus concentration per unit volume can increase 307 with depth into the aggregates as additional aggregates collect. The model neglects the vertical 308 advection of fluid associated with layer compaction because diffusion on this depth scale 309 dominates.

310 The carbon profile as concentration is generated by the following equation:

311

312
$$C = C_o * \frac{e^{-K_c * 20 * x}}{e^{-K_v * x}}$$

- K_c (day⁻¹) is the carbon decay rate
- K_v (cm⁻¹) is the volume decay rate
- C_0 is initial carbon concentration in umol/cm³ (because this is per volume, the " V_0 " term is built into C_0)

- 318 2.3.2. The oxygen model parameters and assumptions
- The modeled oxygen profile was treated as steady state in the aggregate layer on the timescale of the layer persistence (weeks to months). This was based on the measured SCOC which would consume the oxygen inventory in the accumulating aggregate layer on a scale of minutes to hours. This assumption was further justified by the likely preexisting gradients into the falling aggregates (after Alldredge and Cohen 1987; Ploug et al., 1997; Ploug and Jorgensen, 1999; Lehto et al., 2014; Steif et al., 2016). Thus the oxygen gradient into and through the aggregate can be calculated with the following equations using MATLab:
- 326 Within the diffuse boundary layer $\emptyset < z \le d$ $\frac{\partial^2 O_2}{\partial z^2} = \emptyset$ (1)

327 For the interval
$$d \le z \le D$$
 $K_{o_2} \frac{\partial^2 O_2}{\partial z^2} = K_c C$ (2)

- 328 where: K_{o_2} is the oxygen diffusion coefficient and K_C is the combined decay rates for the
- different carbon fractions in terms of oxygen consumption.

330 BO₂(
$$z=\emptyset$$
) = bottom water O₂ concentration. (3)

331 At z=d,
$$O_2$$
 and $\frac{\partial O_2}{\partial z}$ are continuous. (4)

$$332 O_2(D) = \emptyset (5)$$

- 334 The depth where oxygen goes to zero, D is the unknown that is determined as the point where
- the sum the carbon consumed above equals the flux across the diffusive boundary layer as
- equation 6.
- The flux of O₂ across the diffusive boundary layer $K_{o_2} \frac{\partial O_2}{\partial z}|_{z=d} = \int_{d-d}^{D-d} K_c C dz$ (6)

Combining equations 1 and 3 for the interval $\emptyset < z < d$

$$340 O_2 = \frac{\partial O_2}{\partial z}|_{z=d} z + BO_2 (7)$$

Evaluating equation 2 under the condition in 4 yields

342
$$O_2(z) = \int_{d-d}^{z} \int_{d-d}^{z'} \frac{K_c}{K_{Q_2}} C dz'' dz' + \frac{\partial O_2}{\partial z}|_{z=d} z + BO_2$$
 (8)

- 343 This is the solution for the oxygen gradient, the unknown is the flux across the floc interface (i.e.
- the SCOC) for the system as a function of the carbon degradation. This can be calculated using
- equations 5, 6, and 8 evaluated at z=D as the sum of the oxygen consumed.
- 346 Assuming steady state:

347
$$\emptyset = \int_{d-d}^{D-d} \int_{d-d}^{z} \frac{K_c}{K_{o_2}} C dz' dz - [(D-d) + d] \int_{d-d}^{D-d} \frac{K_c}{K_{o_2}} C dz + BO_2$$
 (9)

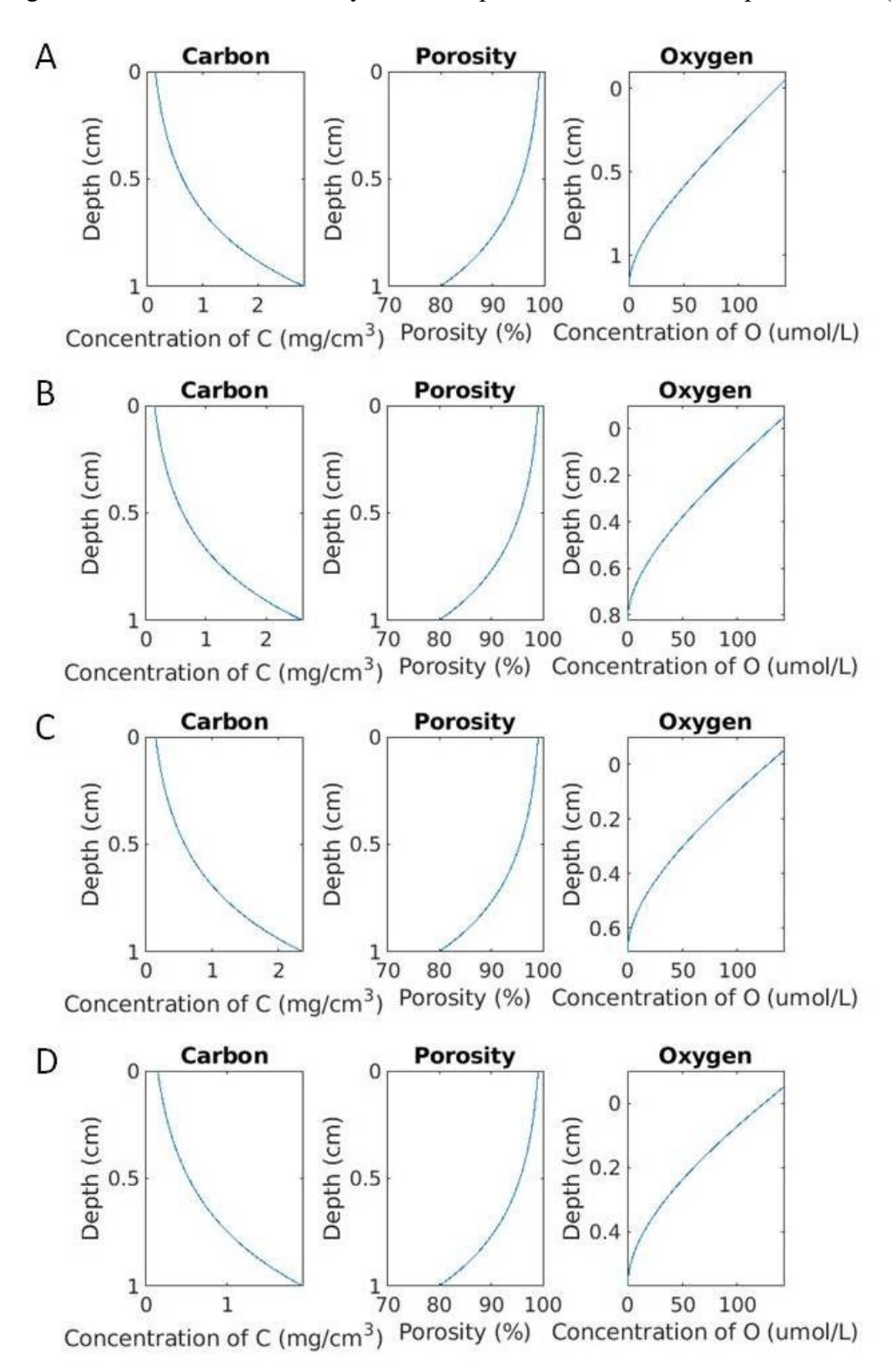
- 348 D-d can be solved using an iterative program in Matlab and then equation 6 yields
- $\frac{\partial O_2}{\partial z}|_{z=d} = \int_{d-d}^{D-d} \frac{K_c}{K_{O_2}} C dz$ and the oxygen profile for depths between d and D can be calculated
- from equation 8. Combining equations 7 and 8 give the overall oxygen profile of

351
$$O(x) = \frac{\partial O_2}{\partial x}|_{z=d} x + BO_2 \quad for \ x \le d$$
 (10)

352
$$O(x) = \int_{d-d}^{x-d} \int_{d-d}^{z} \frac{K_c}{K_{o_2}} C dz' dz + \frac{\partial O_2}{\partial z}|_{z=d} x + BO_2 \quad for \ x > d$$
 (11)

353 Combined model results for the set of parameters in table are presented in Fig. 2.





2.3.3. Oxygen model outputs

The carbon decay model parameters, initial Org C concentration, Org C decay rate and V decay rate, were varied so that the result reproduced the approximate conditions in the aggregate upper layer and the underlying sediments. The suite of resultant Org C profiles required the oxygen decay model to further constrain the parameters used in the Org C model. The constraint on the carbon decay model imposed by the high resolution SCOC data was critical to minimizing the number stable parameter sets. This was particularly useful for the two parameters that were not well constrained by available measurements, the Org C and V decay rates.

The range of Org C decay rates were limited to the lower range of estimated net decay rates calculated for the aggregates, consistent with the "semi-labile" rate measured by Cai et al. (1995). The consistency with the calculated rates is expected as they were constrained by the summed SCOC for each event (see above). However, the agreement with the previous pore water generated rates provides additional support for the validity of the model results (Cai et al., 1995; Dunlap et al., 2016). Model parameter ranges and sources are presented in Table 2.

A synthesis of model results is presented in Table 3 as an indicator of limitations on oxygen mass transfer within the aggregates that fall within the range of measured SCOC for Sta. M. In order to keep SCOC within the measured range, organic carbon to volume ratios at the low end of those measured by Smith et al. (1998) were used. When the organic carbon was restricted to semi-labile fractions the oxygen gradients were more consistent with background sediments after Cai et al., (1995). This suggests that only a fraction of organic carbon delivered as aggregates is degraded using dissolved oxygen on the timescale of the pulse events. The loading of multiple aggregates as a layer may result in compaction and a higher average Org C per unit volume with depth in the layer. Overall, these results are consistent with observations that degradation of the Org C inventory in the aggregate layer is much slower than the duration of the pulse events.

3. Discussion

The results for model runs indicate that the Org C inventory associated with the DA has a reactivity at the low end of measured and predicted values from previous studies. Despite this, the results, when constrained by measured SCOC and the observed aggregate organic carbon

inventories, indicate that oxygen is likely to be completely depleted within the aggregate layer. The high porosity at the aggregate surface and low range of published carbon degradation rates shows that this system is oxygen transport limited rather than carbon limited during pulse events. This is consistent with the relatively low carbon attenuation calculated based on aggregate inventories. Depending on composition and source, individual aggregates maintain oxygen gradients into their interior in the water column (Ploug and Jorgensen, 1999). This is consistent with relatively high microbial abundance in aggregates (as marine snow, Bowen et al., 1993). These results suggest a significant fraction of the aggregate POC inventory may have "aged" in the upper water column prior to aggregation into rapidly falling particles.

386

387

388

389

390

391

392

393

394

395

396

397

398

399

400

401

402

403

404

405

406

407

408

409

410

411

412

413

414

415

Two phenomena that mediate and characterize POC pulses in the water column, particle size and reactivity, are primary controls on oxygen availability at the surface of the settled aggregate layer. In turn, both of these pulse attributes lead to reduced carbon attenuation. Organic carbon degradation as attenuation in the water column is a function aggregate size as it affects particle residence time (Goldthwait et al., 2005). Particles of marine snow host an abundant microbial community that far exceeds the cell density of surrounding waters (Bowen et al., 1993), thus kinetic limitations on degradation are related to oxidant availability and organic carbon reactivity. Aggregate size mediates settling rates and hence residence times (Alldredge and Gotschalk, 1990; Alldredge and Passow, 1994) and should then covary with organic carbon "quality" or "age" within the particles. The relatively short elapsed times between surface productivity events and appearance of aggregates at the sea floor (Smith et al., 2018) are consistent with larger, faster settling particles. However SCOC and model results suggest that fast settling particles do not necessarily contain more labile carbon. The persistence of the pulse events and sometimes longer duration of aggregate accumulation at the sea floor is consistent with deposition of aggregates of aged particles. Aggregation implies capture of particle inventories to form larger particles regardless of the age of those particles. The intensity and duration of the aggregate deposition event that preceded pulse event 5 and continued through pulse event 6 indicates export of an extensive and mature inventory of POC (Smith et al., 2018). The limited response in SCOC, suggests that the large Org C inventory delivered in 2017 was not rapidly remineralized by the ambient microbial community using oxygen, consistent with model results. These major aggregate deposition events include large inventories of relatively

refractory or "aged" Org C under conditions that support reduced attenuation of the POC flux at the sea floor.

The modeled limitation on oxygen transport at the sediment-water interface when compared to the water column observations is consistent with the change in surface area and reduction of advective water flow around particles (Ploug and Jorgensen, 1999). In laboratory and model studies, Lehto et al., (2014) have shown that single aggregates (2 mm diameter) settled on a sediment surface generated a persistent anoxic microenvironment in proximity to the aggregate. The accumulation of aggregates that produce layers with lifetimes of days to months are likely to produce persistent anoxic conditions. Figure 3 provides a conceptual extension of the result of Ploug and Jorgensen (1999) and Lehto et al., (2014) as multiple aggregate particles settle. In simple terms, oxygen transport into degrading particles as they transition from advective three-dimensional space in the water column to diffusive two-dimensional space at the sediment surface has the potential to drive rapid shoaling of the oxygen profile.

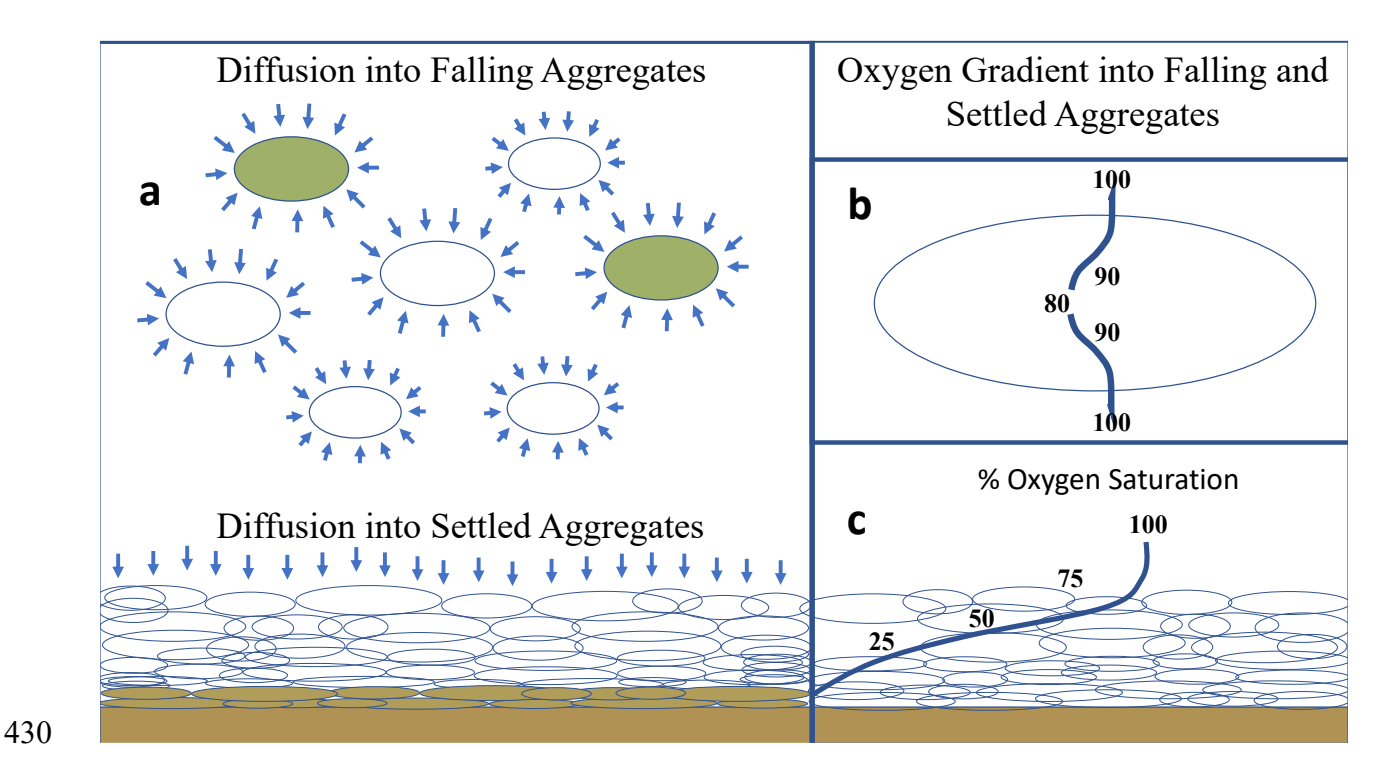


Fig. 3. Conceptual model of oxygen transport and consumption in settling aggregates (a), as individual aggregates in the water column (b) and as they settle (c), after Ploug and Jorgensen (1999).

436

437

438

439

440

441

442

443

444

445

446

447

448

449

450

451

452

453

454

455

456

457

458

459

460

461

462

463

The oxygen gradients in falling aggregate particles decrease from the periphery of the diffusive boundary to the interior, but do not decrease to near depletion (Ploug and Jorgensen, 1999). This is consistent with high carbon content, but low carbon concentration per unit volume. In contrast, Alldredge and Cohen (1987) showed that microbial degradation in fecal pellets within marine snow led to anoxia, presumably associated with lower porosity of the pellets. Similarly, once the particle falls on a surface, the oxygen gradient changes to establish a new steady state very rapidly, resulting in a sustained sharp gradient down to less than 10% oxygen saturation for a particle on the scale of a few mm (Ploug and Jorgensen, 1999; Lehto et al., 2014). These observations are consistent with results for the model of porosity loss in the carbon degradation model to drive the oxygen consumption model for Sta. M.

3.1. Significance of the model results in the context of the Sta. M time series

Smith et al. (2018) identify a significant increase in total POC export and export as pulse events between 2011 and 2018 compared to their overall 30-year time series. The fraction of the POC flux that occurred as six pulse events was 43% of the total measured in traps 600 mab (3400 m) during that period (Smith et al., 2018). All of the identified pulse events also resulted in major aggregate deposition events. Time series data were used to calculate the fraction of the pulse POC fluxes that occurred under oxygen limited conditions in the resulting aggregate layer (i.e. when more than 47% of the sediment surface was covered with aggregates). For pulse events 1in 2012 and 5 and 6 in 2017, the POC flux resulting in significant aggregate cover accounted for about 80% of the total POC flux to the 3400 m traps for those years. For pulse events 2, 3, and 4 in 2016, ~70% of the annual flux events occurred during significant aggregate cover. While pulses of aggregate deposition have been shown to increase grazing by megafauna, their contribution to aggregate Org C consumption is relatively low based on tracer studies (Lauerman et al., 1997). However, increased bioturbation associated with these events (after Lauerman et al., 1997; Laureman and Kaufman, 1998) may increase the rate that pulses of Org C are incorporated into underlying sediments prior to their degradation. Overall, an increasing fraction of aggregate material will undergo diagenesis under low to zero oxygen conditions. The duration of the DA cover event in 2017 suggest that aggregation of the water column inventory of marine snow can drive significant C org deposition and associated shifts in sediment redox

conditions beyond the timescales of the pulse events. A persistent shift in sediment redox conditions may, in turn, increase anaerobic nitrogen turnover (Steif et al., 2016). Thus, the events identified in the study by Smith et al. (2018) probably underestimate the impact of pulses of aggregates reaching abyssal sediments. These findings reflect processes that support enhanced organic carbon burial as low carbon attenuation upon settling at the sediment-water interface. As pulse carbon makes up an increasing fraction of the total abyssal carbon, conditions that lead to lower attenuation should support a significant increase in carbon burial.

4. Conclusions

Numerous studies indicate that aggregate formation has a disproportionate role in export of organic carbon to abyssal depths, mediating carbon attenuation and net delivery to the sediments. In turn, the properties of aggregates that mediate pulse events, large size and rapid settling also limit oxygen utilization at the sea floor. These microhabitats support a rich microbial community that can be sustained through the rapid change in redox environment associated with the thick, organic carbon rich aggregate layers at the sea floor. The general increase in duration and intensity of pulse events is accompanied by the reduced attenuation for much of the large Org C inventory delivered as detrital aggregates to Sta. M sediments. The relationship between changes in surface ocean dynamics and the increasing frequency of pulse events at Sta. M offer insight into the future of carbon export intensity in the CCE. These conditions are not likely to be confined to the CCE, suggesting that early diagenesis and carbon preservation in deep ocean sediments may be much more dynamic than previously considered. The associated preservation of organic carbon as reduced attenuation in pulse affected sediments require a reassessment of the abyssal sediment carbon sink.

Acknowledgements

The authors would like to thank the Smith group past and present for their effort in maintaining the Sta. M time series and their generosity in sharing data, photos, and ideas. The authors would also like to thank Dan Rudnick, who provided the first iteration of the oxygen

- 494 model that was later adapted for this application. This work was also partially funded by NSF
- 495 OCE 1559274, OCE 1829333 and the David and Lucile Packard Foundation.

497 References in GCA format

498

- Agusti, S., Gonza'lez-Gordillo, J.I., Vaque', D., Estrada, M., Cerezo, M. I., Salazar, G., Gaso, J.
- M., Duarte, C. M. 2015, Ubiquitous healthy diatoms in the deep sea confirm deep carbon
- injection by the biological pump, Nature Comm. DOI: 10.1038/ncomms8608.

502

- 503 Alldredge, A.L. and Cohen, Y. (1987) Can Microscale Chemical Patches Persist in the Sea -
- Microelectrode Study Of Marine Snow, Fecal Pellets. Science 235, 689-691.

505

- Alldredge, A.L. and Gotschalk, C. (1988) In-situ Settling Behavior of Marine Snow. Limnology
- 507 and Oceanography 33, 339-351.

508

- Alldredge, A.L. and Gotschalk, C.C. (1990) The Relative Contribution of Marine Snow of
- 510 Different Origins to Biological Processes in Coastal Waters. Continental Shelf Research 10, 41-
- 511 58.

512

- Alldredge, A.L., Passow, U. and Logan, B.E. (1993) The Abundance and Significance of a Class
- of Large, Transparent Organic Particles in the Ocean. Deep-Sea Research Part I-Oceanographic
- 515 Research Papers 40, 1131-1140.

516

- Alldredge, A.L., Passow, U. (1994) Distribution, size and bacterial-colonization of transparent
- exopolymer particles (tep) in the ocean. Mar. Ecol. Prog. Series 113 (2) 185-198.

519

- Alldredge, A.L. and Silver, M.W. (1988) Characteristics, Dynamics and Significance of Marine
- 521 Snow. Progress in Oceanography 20, 41-82.

- Baldwin, R.J., Glatts, R.C. and Smith, K.L. (1998) Particulate matter fluxes into the benthic
- boundary layer at a long time-series station in the abyssal NE Pacific: composition and fluxes.
- Deep-Sea Research Part Ii-Topical Studies in Oceanography 45, 643-665.

- 527 Beaulieu, S.E. and Smith, K.L. (1998) Phytodetritus entering the benthic boundary layer and
- aggregated on the sea floor in the abyssal NE Pacific: macro- and microscopic composition.
- Deep-Sea Research Part Ii-Topical Studies in Oceanography 45, 781-816.

530

- Bett, B. J., Malzone, M. G., Narayanaswamy, B. E., Wigham. B. D. (2001) Temporal variability
- in phytodetritus and megabenthic activity at the seabed in the deep Northeast
- Atlantic. Progress in Oceanography 50, 349–368.

534

- Billett, D.S.M., Lampitt, R.S., Rice, A.L. and Mantoura, R.F.C. (1983) Seasonal Sedimentation
- of Phytoplankton to the Deep-Sea Benthos. Nature 302, 520-522.

537

- Boetius, A., Albrecht, S., Bakker, K., Bienhold, C., Felden, J., Fernández-Méndez, M.,
- Hendricks, S., Katlein, C., Lalande, C., Krumpen, T., Nicolaus, M., Peeken, I., Rabe, B.,
- Rogacheva, A., Rybakova, E., Somavilla, R., Wenzhöfer., F. (2013) Export of algal biomass
- from the melting Arctic Sea ice. *Science* 339, 1430-1432.

542

- Bowen, J. D., Stolzenbach, K. D., Chisholm, S. W. (1993) Simulating bacterial clustering around
- phytoplankton cells in a turbulent ocean. *Limnol. Oceanogr.* 38(1), 36-51

545

546547

- Buesseler, K.O. and P.W. Boyd (2009) Shedding light on processes that control particle export
- and flux attenuation in the twilight zone of the open ocean, *Limnol. Oceanogr.* 54(4): 1210–1232

550

- Buesseler, K.O. (1998) The decoupling of production and particulate export in the surface ocean,
- 552 Global Biogeochem. Cycles, 12: 297-310

- Buesseler K.O., T.W. Trull, D.K. Steinberg, M.W. Silver, D.A. Siegel, S.-I. Saitoh, C.H.
- Lamborg, P.J. Lam, D.M. Karl, N.Z. Jiao, M.C. Honda, M. Elskens, F. Dehairs, S.L. Brown,
- P.W. Boyd, J.K.B. Bishop, R.R. Bidigare (2008) VERTIGO (VERtical Transport In the Global
- Ocean): A study of particle sources and flux attenuation in the North Pacific. Deep Sea Res. II
- 558 55:1522–1539.

- Cai, W.J., Reimers, C.E. and Shaw, T. (1995) Microelectrode Studies of Organic-Carbon
- Degradation and Calcite Dissolution at a California Continental Rise Site. Geochimica Et
- 562 Cosmochimica Acta 59, 497-511.

563

- Dunlop, K.M., van Oevelen, D., Ruhl, H.A., Huffard, C.L., Kuhnz, L.A. and Smith, K.L., Jr.
- 565 (2016) Carbon cycling in the deep eastern North Pacific benthic food web: Investigating the
- effect of organic carbon input. Limnology and Oceanography 61, 1956-1968.

567

- 568 Emerson, S., Fischer, K., Reimers, C. and Heggie, D. (1985) Organic-Carbon Dynamics and
- Preservation in Deep-Sea Sediments. Deep-Sea Research Part a-Oceanographic Research Papers
- 570 32, 1-21.

571

- Fabiano, M., Pusceddu, A., Dell'Anno, A., Armeni, M., Vanucci, S., Lampitt, R.S., Wolff, G.A.
- and Danovaro, R. (2001) Fluxes of phytopigments and labile organic matter to the deep ocean in
- 574 the NE Atlantic Ocean. Progress in Oceanography 50, 89-104.

575

- 576 Giering, S.L.C., Sanders, R., Lampitt, R.S., Anderson, T.R., Tamburini, C., Boutrif, M., Zubkov,
- 577 M.V., Marsay, C.M., Henson, S.A., Saw, K., Cook, K. and Mayor, D.J. (2014) Reconciliation of
- 578 the carbon budget in the ocean's twilight zone. Nature 507, 480-483.

579

- Goldthwait, S.A., Carlson, C.A., Henderson, G.K. and Alldredge, A.L. (2005) Effects of physical
- fragmentation on remineralization of marine snow. Marine Ecology Progress Series 305, 59-65.

- Hammond, D.E., McManus, J., Berelson, W.M., Kilgore, T.E. and Pope, R.H. (1996) Early
- diagenesis of organic material in equatorial Pacific sediments: Stoichiometry and kinetics. Deep-
- Sea Research Part Ii-Topical Studies in Oceanography 43, 1365-1412.

- Henson, S.A., Sanders, R., Madsen, E., Morris, P.J., Le Moigne, F. and Quartly, G.D. (2011) A
- reduced estimate of the strength of the ocean's biological carbon pump. Geophysical Research
- 589 Letters 38.

590

- KiBrboe, T., Hansen, J. L. S., Alldredge, A. L., Jackson, G. A., Passow, U., Dams, H. G.,
- Drapeaus, D. T., Waite, A., Garcia, C. M., 1996 Sedimentation of phytoplankton during a
- diatom bloom: Rates and mechanisms. J. Mar. Res., 54, 1123-1148.

594

- Kiriakoulakis, K., Stutt, E., Rowland, S.J., Vangriesheim, A., Lampitt, R.S. and Wolff, G.A.
- 596 (2001) Controls on the organic chemical composition of settling particles in the Northeast
- 597 Atlantic Ocean. Progress in Oceanography 50, 65-87.

598

- Lampitt, R.S. (1985) Evidence for the Seasonal Deposition of Detritus to the Deep-Sea Floor and
- its Subsequent Resuspension. Deep-Sea Research Part a-Oceanographic Research Papers 32,
- 601 885-897.

602

- Lampitt, R.S., Bett, B.J., Kiriakoulakis, K., Popova, E.E., Ragueneau, O., Vangriesheim, A. and
- Wolff, G.A. (2001) Material supply to the abyssal seafloor in the Northeast Atlantic. Progress in
- 605 Oceanography 50, 27-63.

606

- Lampitt, R.S., Salter, I., de Cuevas, B.A., Hartman, S., Larkin, K.E. and Pebody, C.A. (2010)
- 608 Long-term variability of downward particle flux in the deep northeast Atlantic: Causes and
- trends. Deep-Sea Research Part II-Topical Studies in Oceanography 57, 1346-1361.

610

- Lauerman, L. and Kaufmann, R.S. (1998) Deep-sea epibenthic echinoderms and a temporally
- 612 varying food supply, *Deep Sea Res.* II 45: 817-842-779.

- 614 Lauerman, L., Smoak, J. M., Shaw, T. J., Moore, W., Smith K. L., (1997). ²³⁴Th and ²¹⁰Pb
- evidence of rapid ingestion of settling particles by mobile epibenthic megafauna in the abyssal
- 616 NE Pacific. *Limnol. Oceanogr.* 42(3), 589-595 (1997).

- 618 Laws, E.A., Falkowski, P.G., Smith, W.O., Ducklow, H. and McCarthy, J.J. (2000) Temperature
- effects on export production in the open ocean. Global Biogeochemical Cycles 14, 1231-1246.

620

- 621 Lehto, N., Glud, R. N., Norði, G. A., Zhang, H., Davison, W., (2014)
- Anoxic microniches in marine sediments induced by aggregate settlement: biogeochemical
- dynamics and implications. *Biogeochemistry*, 119, 307-327

624

- Marsay, C.M., Sanders, R.J., Henson, S.A., Pabortsava, K., Achterberg, E.P. and Lampitt, R.S.
- 626 (2015) Attenuation of sinking particulate organic carbon flux through the mesopelagic ocean.
- Proceedings of the National Academy of Sciences of the United States of America 112, 1089-
- 628 1094.

629

- Moradi, N., Liu, B., Iversen, M., Kuypers, M.M., Ploug, H. and Khalili, A. (2018) A new
- mathematical model to explore microbial processes and their constraints in phytoplankton
- colonies and sinking marine aggregates. Science Advances 4, DOI: 10.1126/sciadv.aat199

633

- Ploug, H., Kuhl, M., Buchholz-Cleven, B. and Jorgensen, B.B. (1997) Anoxic aggregates an
- ephemeral phenomenon in the pelagic environment? Aquatic Microbial Ecology 13, 285-294.

636

- Ploug, H. and Jorgensen, B.B. (1999) A net-jet flow system for mass transfer and microsensor
- studies of sinking aggregates. Marine Ecology Progress Series 176, 279-290.

639

- Ploug, H. and Passow, U. (2007) Direct measurement of diffusivity within diatom aggregates
- containing transparent exopolymer particles. Limnology and Oceanography 52, 1-6.

- Ploug, H., Iversen, M.H. and Fischer, G. (2008) Ballast, sinking velocity, and apparent
- diffusivity within marine snow and zooplankton fecal pellets: Implications for substrate turnover
- by attached bacteria. Limnology and Oceanography 53, 1878-1886.

- Prairie, J.C., Ziervogel, K., Camassa, R., McLaughlin, R.M., White, B.L., Dewald, C. and
- Arnosti, C. (2015) Delayed settling of marine snow: Effects of density gradient and particle
- properties and implications for carbon cycling. Marine Chemistry 175, 28-38.

650

- Riley J.S., R. Sanders, C. Marsay, F.A.C. Le Moigne, E.P. Achterberg and A. J. Poulton (2012)
- The relative contribution of fast and slow sinking particles to ocean carbon export. *Global*
- 653 Biogeochem. Cycles, 26: GB1026, doi:10.1029/2011GB004085.

654

- Shaw T. J., J.M. Smoak and L. Lauerman (1998) Scavenging of ²³⁴Th, ²³⁰Th, and ²¹⁰Pb by
- particulate matter in the deep waters of the California continental margin, *Deep Sea Res.* II 45:
- 657 763-779.

658

- 659 Smith, K.L., Jr., Ruhl, H.A., Huffard, C.L., Messie, M. and Kahru, M. (2018) Episodic organic
- carbon fluxes from surface ocean to abyssal depths during long-term monitoring in NE Pacific.
- Proceedings of the National Academy of Sciences of the United States of America 115, 12235-
- 662 12240.

663

- 664 Smith, K.L., Baldwin, R.J., Glatts, R.C., Kaufmann, R.S. and Fisher, E.C. (1998) Detrital
- aggregates on the sea floor: Chemical composition and aerobic decomposition rates at a time-
- series station in the abyssal NE Pacific. Deep-Sea Research Part Ii-Topical Studies in
- 667 Oceanography 45, 843-880.

668

- 669 Smith, K.L., H.A. Ruhl, M. Kahru, C.L. Huffard and A.D. Sherman (2013) Deep ocean
- 670 communities impacted by changing climate over 24 y in the abyssal northeast Pacific Ocean,
- 671 Proc. Natl. Acad. Sci. USA. 110:19838-19841

- 673 Smith, K.L., A.D. Sherman, C.L. Huffard, P.R. McGill, R. Henthorn, S. Von Thun, H.A. Ruhl,
- M. Kahru and M.D. Ohman (2014) Large salp bloom export from the upper ocean and benthic
- 675 community response in the abyssal northeast Pacific: Day to week resolution, *Limnol. Oceanogr.*
- 676 59:745-757

- 678 Smith, K.L., C.L. Huffard, A.D. Sherman and H.A. Ruhl (2016) Decadal change in sediment
- 679 community oxygen consumption in the abyssal northeast Pacific, Aquat. Geochem. 22(5-6):401-
- 680 417.

681

- 682 Smith, K.L., Jr, A.D. Sherman, P.R. McGill, R.G. Henthorn, J. Ferreira, C.L. Huffard (2017)
- 683 Evolution of monitoring an abyssal time-series station in the Northeast Pacific over 28 years.
- 684 *Oceanography* 30 (4): 72-81

685

- 686 Stief, P., Kamp, S., Thamdrup, B., Glud, R. N. (2016)
- Anaerobic Nitrogen Turnover by Sinking Diatom Aggregates at Varying Ambient Oxygen
- 688 Levels. Front. Microbiol. 7:98. doi: 10.3389/fmicb.2016.00098

689

- 690 Stukel, M.R., L.I. Aluwihare, K.A. Barbeau, A.M. Chekalyuk, R. Goericke, A.J. Miller, M.D.
- Ohman, A. Ruacho, H. Song, B.M. Stephens and M.R. Landry (2017) Mesoscale ocean fronts
- enhance carbon export due to gravitational sinking and subduction, *Proc. Natl. Acad. Sci. USA*.
- 693 114:1252-1257.

694

- Witbaard, R., Dunieveld, G.C.A., Van der Weele, J.A., Berghuis, E.M. and Reyss, J.P. (2000)
- The benthic response to the seasonal deposition of phytopigments at the Porcupine Abyssal Plain
- in the North East Atlantic. *Journal of Sea Research* 43, 15-31.

698

700 Table 1. Pulse attenuation based on sediment trap POC flux and aggregate inventory

| Pulse Event # | 1 | 2 | 3 | 4 | 5 | 6 |
|--|-----------|--------------|-----------|-----------|-----------|-----------|
| POC trap flux per event mg C m ⁻² | 1480 | 590 (4/9/16- | 1010 | 1210 | 1180 | 2600 |
| (Smith et al., 2018) | (3/21/12- | 4/28/16) | (6/18/16- | (9/26/16- | (6/23/17- | (9/1/17- |
| | 5/19/12) | | 7/7/16) | 11/4/16) | 7/22/17) | 11/19/17) |

| Attenuation of EF at Sediment Traps | 77% | 72% | 57% | 76% | 69% | 74% |
|-------------------------------------|------------|------------|------------|---------|-----------|-----------|
| (percent regenerated) | | | | | | |
| Half-life of EF pulse and lag time | 19: 40 | 5: 10 | 8: <10* | 5: <10 | 6: <10 | 10: 20 |
| (both in days) | | | | | | |
| Average Detrital Aggregate Org C | 1362 (4/3- | 983 (4/23- | 1668 (7/2- | 894 | 3433 | 2727 |
| Inventory mg C m ⁻² | 7/16/12) | 5/7/16) | 7/15/16) | (10/11- | (6/23/17- | (9/1/17- |
| | | | | 11/18) | 7/22/17) | 11/19/17) |
| Attenuation of EF reaching the Sea | 79% | 53% | 28% | 76% | 10% | 73% |
| Floor (as DA inventory) | | | | | | |
| Half-life of Aggregate Inventory | 46 | 62 | 83 | 46 | 46 | 129 |
| based on SCOC (days) | | | | | | |

*The 10-day resolution of the trap collections was used as a minimum when no clear lag time

was detected.

Table 2. Model parameters

| <u>Parameter</u> | | Sources |
|---|-------------|----------------------------------|
| Diffusive Boundary Layer (cm) | 0.01-0.05 | Ploug et al., 1997 |
| DA carbon degradation rate (day ⁻¹) | 0.001-0.015 | Table 1 |
| DA volume decay rate (day-1) | 3 | Porosity Gradient |
| Flock thickness (cm) | 0.5-1.0cm | Smith et al., 1998, Figure 1 |
| Carbon Inventory | ~1600 | Smith et al., 1998; 2018 Table 1 |
| Oxygen diffusion coefficient (cm²/day) | 1.04 | Emerson et al., 1985 |

 Table 3. A subset of model results that demonstrate the impact of carbon degradation rates and volume decay rate as SCOC. Carbon inventory is calculated for the upper 0.5 cm as in Table 3 for comparison. Results presented for rates >0.005 run at the average organic carbon concentration exceed measured SCOC.

| Selected Model Runs | Org C Decay Rate (d ⁻¹) | SCOC (mgOrgC m ⁻² d ⁻¹) | Org C inventory (mg C m ⁻²) |
|---------------------|-------------------------------------|---|---|
| Figure 2a | 0.001 | 16.1 | 1660 |
| Figure 2b | 0.005 | 24.6 | 1620 |
| Figure 2c | 0.010 | 30.2 | 1570 |
| Figure 2d | 0.020 | 37.5 | 1480 |